Eur. Phys. J. Special Topics **166**, 67–71 (2009)

DOI: 10.1140/epjst/e2009-00880-4

THE EUROPEAN PHYSICAL JOURNAL SPECIAL TOPICS

Regular Article

Capillarity induced folding of elastic sheets

C. Py[1,a], P. Reverdy[2], L. Doppler[3], J. Bico[3], B. Roman[3], and C.N. Baroud[2]

[1] Matière et Systèmes Complexes, UMR CNRS 7057, Université Paris Diderot, Paris, France
[2] Laboratoire d'Hydrodynamique (LadHyX) and Département de Mécanique, École Polytechnique, UMR CNRS 7646, Palaiseau, France
[3] Physique et Mécanique des Milieux Hétérogènes, ESPCI, Paris 6, Paris 7, UMR CNRS 7635, Paris, France

Abstract. Surface tension forces induced by a liquid droplet are used to bend thin elastic sheets into three dimensional structures. The resulting 3D shape may be controlled by tailoring the initial cut of the sheet. We derive the criterion for folding from a balance between elastic and capillary effects and compare it with the experiments. This mechanism can be used for fabrication of three-dimensional micro- or nano-scale objects through the self-folding of planar templates.

1 Introduction

Capillary forces usually do not have noticeable effects on solids at human scales, however they become dominant as the surface effects start overcome volumetric effects, when the scale of interest becomes sub-millimetric. Although they allow insects to walk on water [8], surface forces are at the origin of fabrication difficulties in MEMS and nano-technologies. Indeed microstructures are known to collapse or to stick together in humid environments, leading to irreversible damage [9]. Conversely, it was recently shown that surface tension forces could be used for the self-assembly of rigid microstructures into complex objects [2]. For examples rigid pannels, articulated around weakened junctions that act like hinges, are folded up by surface tension forces when a solder drop is melted [1,3]. In this case the control of the different assembled shapes relies on the precise engineering of the hinges. In this paper, we report the spontaneous folding of featureless elastic sheets on which a water drop is deposited. This folding leads to robust and precise three dimensional structures that may be controlled by tayloring the initial planar cut. In a second part we describe the physical ingredients at play and present a criterion for the folding to occur.

2 Wrapping liquid droplets

Our experiments were conducted using polydimethylsiloxane (PDMS) membranes. The PDMS (Dow corning Sylgard 184, 10:1 polymer/curing agent mix) was spin coated at 24 °C on a glass microscope slide, at rotation rates of 1000–2000 rpm. Once the PDMS was cured, this resulted in sheets with thickness in the range $80 - 40\,\mu$m.

During a typical experiment, a geometric shape is manually cut out from the PDMS layer and placed on a super-hydrophobic surface. A drop of water, of volume $1 - 80\,\mu$L, depending on the membrane size, is deposited on the PDMS, making sure that the water reaches all the corners of the flat sheet. The water is then allowed to evaporate at room temperature and a time lapse

[a] e-mail: charlotte.py@univ-paris-diderot.fr

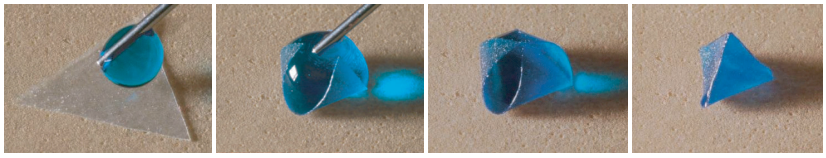

Fig. 1. Wrapping of a drop of water with a triangular PDMS sheet, leading to a pyramid.

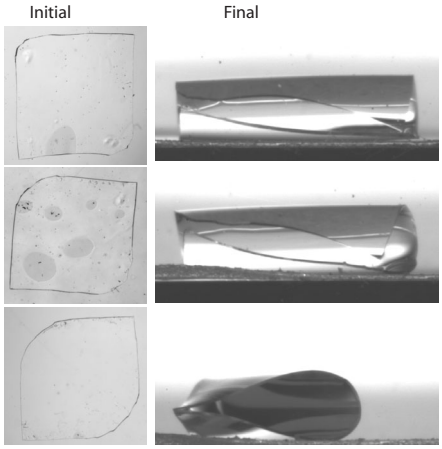

Fig. 2. Transition between folding modes of a square sheet as two opposite corners are rounded. For a nearly square sheet, the final shape is a rectangle, switching to a triangle beyond a critical reduction.

sequence of images is taken of the membrane/drop pair. As the water volume decreases from its initial value to complete evaporation, the surface tension of the liquid pulls the sheet around smaller volumes, thus increasingly curving it. Sufficiently thin sheets eventually encapsulate the liquid with a shape that depends on the initial cut of the membrane.

Figure 1 illustrates this capillary wrapping in the case of a triangular sheet. As a drop is deposited, the corners fold towards the center and eventually join, which leads the sheet to seal into a tetrahedral pyramid. Further evaporation, occuring at slower rates, would lead to the buckling of the pyramid walls due to negative internal pressure. However, one may freeze (or polymerize) the encapsulated liquid, therefore fixing the desired shape in place. Different 3D shapes can be obtained by tailoring the initial sheet geometry: for instance, cubes and spheres are formed from cross and flower shapes [4]. Finally, small perturbations of the initial shape may also be used to yield different final states. In particular, rounding-off two opposite corners of a square sheet leads to the membrane closing along its diagonal rather than parallel to the sides (Fig. 2). These experiments suggest that a wide variety of final shapes may be achieved through careful tuning of the initial flat template.

3 Combining elasticity and capillarity

3.1 The elastocapillary length

We now describe the physical ingredients responsible for the capillary wrapping. The folding of the membrane around the drop reduces the liquid-air area and thus the surface energy of the drop, at the cost of increasing the elastic energy of the membrane. The capillary origami is therefore governed by a competition between these two effects, which may be illustrated by a simple experiment. Let a thin plate of length L come into contact with a rigid cylinder with radius R coated with a wetting liquid (Fig. 3a). If the plate is sufficiently compliant, it folds around the cylinder (Fig. 3b), but stays flat otherwise (Fig. 3a). The surface energy gained in the first case, γL (per unit width, γ being the surface tension), must overcome the increase in

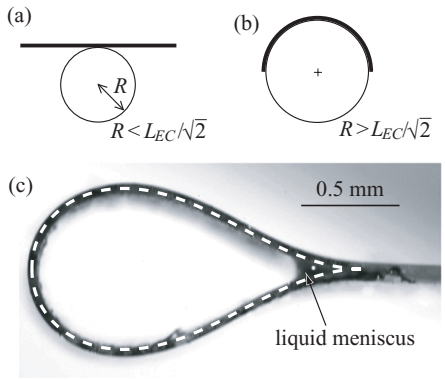

Fig. 3. (a,b) Wrapping of a cylinder coated with a wetting liquid by an elastic sheet provided the radius of the cylinder is larger than the elastocapillary length L_{EC}. (c) Experimental image of a loop of PDMS held by a meniscus of ethanol, and comparison with the theoretical shape (dashed curve).

bending energy, $BL/2R^2$ where $B = Eh^3/12(1-\nu^2)$ is the bending stiffness (E is the Young's modulus, ν the Poisson's ratio and h the plate thickness) [7]. The ratio of these antagonist terms gives the radius above which wrapping occurs, $R = L_{EC}/\sqrt{2}$, where

$$L_{EC} = \sqrt{B/\gamma} \tag{1}$$

is refered to as the *elastocapillary length* [6]. L_{EC} corresponds to the typical radius of curvature that capillary forces may generate on a solid with given bending rigidity. This scaling argument indicates that the critical size L_{crit} beyond which the sheet totally wraps the liquid droplet should be proportional to L_{EC}, the only length scale present in the problem.

The elastocapillary length can be directly measured through a calibration experiment rather than by estimating each parameter in Eq. 1 which would produce large errors. The experiment consists in depositing a drop of wetting liquid onto a very long strip of PDMS that folds over into a loop with a self-contacting tail. The drop is allowed to evaporate and we consider the late stage, when only a small meniscus still holds the loop together (Fig. 3c). This 2D equilibrium state may be described by a simple theory where the shape of the loop is governed by planar rod elasticity and the radius of curvature at the contact point is imposed by capillarity, as $\kappa_c = \sqrt{2}/L_{EC}$ (details are given in [4]). Solving the problem leads to the theoretical shape of the loop which depends only on L_{EC}. The elastocapillary length L_{EC} can therefore be determined by scaling the numerical solution to fit the experimental shape, as shown in Fig. 3c. Excellent agreement is obtained between the numerical and experimental shapes with, in practice, only the width of the loop (theoretical value $0.89L_{EC}$) being necessary to determine L_{EC}.

3.2 Criterion for encapsulation

Once the elastocapillary length was measured for different membrane thicknesses, the criterion for droplet encapsulation was determined. To do so, we considered the case of square PDMS sheets. Depositing a drop of water on such sheet initially leads to the bending of the four corners towards the center of the sheet (mode-4), Fig 4. For thin enough sheets, this bending mode becomes unstable as the drop volume decreases further and the shape rapidly switches to a mode-2 state; in this state, the corners are attracted to each other two by two and the flat central region disappears, giving rise to a quasi-cylindrical shape (second image in Fig 4-right). As the drop volume decreases further, the approaching edges eventually touch and a water-filled tube is formed. Finally, the water evaporates completely and the tube grows into a loop whose cross-section is similar to the shape shown in Fig. 3c.

A different scenario is observed for membranes of smaller size or larger thickness (Fig. 4-left). As the stiffness increases, the forces generated by surface tension become insufficient to

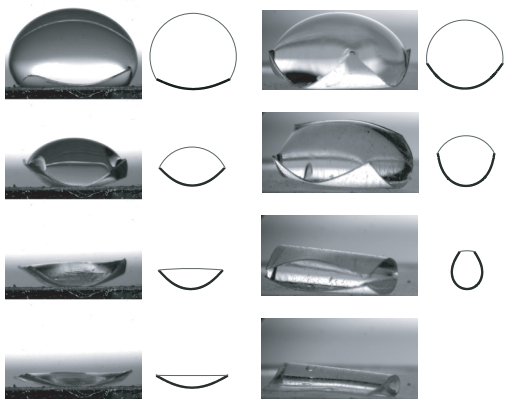

Fig. 4. Complete encapsulation of a drop of water with a square sheet (right) or reopening (left) depending on the size of the sheet with respect to the elastocapillary length, and comparison with the theory. The numerical simulation stops as soon as closure is reached.

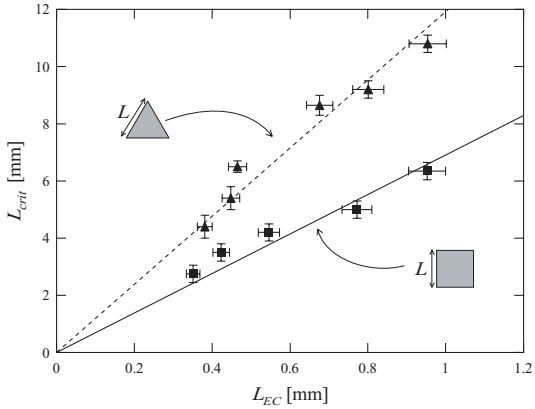

Fig. 5. Critical length for folding vs. elasto-capillary length: black squares: square sheets, black triangles: triangular sheets, lines: linear regressions expected from dimensional analysis.

achieve complete closure: after going through similar initial stages as for thin PDMS layers, a maximum bending of the sheet is produced after which it reopens again, never having produced an encapsulated drop. The final state is therefore a planar sheet covered by a thin film of liquid which quickly evaporates.

Both types of behavior are qualitatively reproduced in Fig. 4 by a numerical solution of a 2D model presented in [4], in which an elastic rod is bent by pressure and surface tension forces.

For each membrane thickness, the minimum length for encapsulation L_{crit} was determined for square and triangular membrane shapes and compared to the associated elastocapillary length (Fig. 5). The experimental results are consistent with a linear relationship between L_{crit} and L_{EC} as expected from dimensional analysis. Based on this, a linear fit of the data leads to $L_{crit} = 7.0L_{EC}$ for squares and $L_{crit} = 11.9L_{EC}$ for triangles (Fig. 5).

The transition between the two scenarios (encapsulation versus reopening) was found in the theoretical model for $L_{crit} = 3.54L_{EC}$, which is of the same order but below the value experimentally obtained for the square membranes. An improved model should include 3D effects and stretching. The actual 3D situation is indeed more complex due for instance to the geometrical incompatibility of wrapping a sphere with a planar sheet (Gauss's *theorema egregium*), which not only involves bending but also stretching energy [5].

In summary, three dimensional millimetre scale objects are produced from flat membranes through the interaction of elasticity and capillarity. The limitation on the minimal size for folding is determined by the elastocapillary length (Eq. 1) which scales as the sheet thickness

$h^{3/2}$. This scaling is favorable to miniaturization since thinner membranes lead to much smaller critical lengths, leading to promising applications in micro-fabrication. Finally, the final shapes are shown to be highly reproducible and to depend on the details of the initlal sheet geometry, implying a robust yet general microfabrication technique.

References

1. R.R.A. Syms et al., J. Microelectr. Sys. **12**, 387 (2003)
2. M. Boncheva, D.A. Bruzewicz, G.M. Whitesides, Pure Appl. Chem. **75**, 621 (2003)
3. T.G. Leong, P.A. Lester, T.L. Koh, E.K. Call, D.H. Langmuir, **23**, 8747 (2007)
4. C. Py, P. Reverdy, L. Doppler, J. Bico, B. Roman, C.N. Baroud, Phys. Rev. Lett. **98**, 156103 (2007)
5. S. Alben, M.P. Brenner, Phys. Rev. E **75**, 056113 (2007)
6. J. Bico, B. Roman, L. Moulin, A. Boudaoud, Nature **432**, 690 (2004)
7. L.D. Landau, E.M. Lifshitz, (1986), Oxford, Third
8. D.L Hu, B. Chan, J.W.M. Bush, Nature **424**, 663 (2003)
9. C.H. Mastrangelo, C.H. Hsu, J. Microelectr. Sys. **2**, 33 (1993)